Feasibility analysis of community-based PV systems for residential districts: a comparison of on-site centralized and distributed PV installations

*Reihaneh Aghamolaei[ab], Mohammad Haris Shamsi[a], James O'Donnell[a]

[a]*School of Mechanical and Materials Engineering, UCD Energy Institute, University College Dublin, Belfield, Dublin 4, Ireland.*

[b]*College of Fine arts, University of Tehran, Tehran, Iran.*

**Corresponding Author:*

Email: r.aghamoalei@ut.ac.ir, Reihaneh.aghamolaei1@ucdconnect.ie

Reihaneh Aghamolaei

Ph.D. candidate

School of Mechanical and Materials Engineering,

UCD Energy Institute,

University College Dublin,

Belfield, Dublin 4, Ireland

Feasibility analysis of community-based PV systems for residential districts: a comparison of on-site standalone centralized and distributed PV installations

Abstract

Photovoltaic systems are one of the most promising renewable energy technologies for on-site generation. Most of the techno-economic studies consider distributed standalone photovoltaic generation with little consideration of community-based standalone photovoltaic systems. Location-based case studies are required to provide economic and reliable photovoltaic systems to meet the peak loads of residential neighbourhoods in an optimized manner. This paper devises an integrated evaluation methodology; a combination of white-box energy modelling and black box photovoltaic design optimization. This research uses optimization methods to develop a quantitative optimized model for analysing the opportunities of centralized systems to adequately meet the demands of a residential neighbourhood and support the grid. This analysis includes three metrics including the level of the energy production, reliability of system for peak power and finally the capital cost of implementation in residential districts. Results indicate that the size of a centralized photovoltaic installation is less when compared to distributed installations to support a similar single peak load. The required converter size is reduced for the centralized system owing to the reduced system size. Centralized installations require fewer batteries to store surplus energy produced due to increased interaction of energy flows. Centralized installations are economically more viable than distributed ones.

Keywords

PV Panels; Techno-economic; Feasibility analysis; Homer; Economic Performance; Optimization

Nomenclature and symbols

PV	Photovoltaic
RE	Renewable Energy
DOD	Depth of Discharge
SOC	State of Charge
DC	Direct current
AC	Alternating Current
HOMER	Hybrid Optimization Model for Electric Renewables
RSM	Response Surface Methodology
NPC	Net Present Cost
O&M	Operation and Maintenance
CCSPV	Community-based Centralised Standalone PV
SPV	Stand-alone PV
DSPV	Distributed Standalone PV
NPV	Net Present Value
V_{PV}	Optimum operating point voltage of the PV panel
i_{PV}	Optimum operating point current of the PV panel
V_{mp}	Maximum power voltage
i_{mp}	Maximum power current
V_{OC}	Open-circuit voltage
i_{SC}	Short-circuit current
α_o	Current temperature coefficient
β_o	Voltage temperature coefficient
T_{cell}	Temperature of the PV cell
I_T	Total solar irradiance on tilted panel
I_{st}	Standard solar irradiance (1000 W/m^2)
T_A	Ambient temperature
T_{st}	Standard ambient temperature (25^0C)

1 Introduction

The world has experienced a drastic increase in the growth rate of urban environments resulting in a major population shift to urban areas over the past few decades [1]. Sustainable urban planning has focused on energy-sensitive design as a long-term perspective in local scales since neighbourhoods are one of the most insightful and practical scales for studying energy systems [2]. Existing energy systems are being transformed to increase the penetration of renewable energy sources [3]. Zero energy buildings and neighbourhoods now emerge as viable solutions that can achieve this transformation and balance the annual energy demand using electricity generated from renewable energy sources. Urban planners and researchers have defined initiatives to pave the way for zero energy analysis at the neighbourhood scale [2,4]. Demand and supply balancing with cost and emission analysis are considered as crucial elements of zero energy neighbourhood [5].

Strengthening the potential to produce energy locally is one of the key concepts towards achieving sustainable and zero neighbourhoods [6,7]. PV systems are one of the most promising renewable energy technologies for on-site generation at different scales, especially in local urban areas. High accessibility to solar radiation and increasing residential electricity tariffs justify the use of Standalone PV (SPV) panels [8]. The feasibility of PV application is strongly affected by demand load profiles which significantly change the scenarios for the combination of generation and storage measures [9].

A number of existing studies analysed the potential of localized electricity production at the individual building level [10,11]. These studies analysed different technical, economic and environmental aspects associated with decentralized electricity generation [10,11]. Other researchers analysed the effect of various weather conditions on solar generation in detail and proposed solutions to mitigate reduced generation and unforeseen outcomes [12].

Although the literature on the techno-economic analysis of solar panels has experienced a major boost in the last decade, some issues require additional attention. (1): Most of the techno-economic studies consider DSPV generation with little or no consideration of CCSPV. In fact, centralized PV analysis only exists for large solar PV farms and alongside, the performance of localized PV systems at the neighbourhood scale has not been accounted for. Moreover, analysing the grid interactions of local centralized PV systems are rarely addressed in recent studies [13–15]. (2) Combined systems with complicated components are not sufficiently addressed [16]. Optimization strategies considering storage systems have to be developed

based on distinctive characteristics, practical needs, and uncertainties that exist at different locations. Therefore, location-based case studies are required to provide economic and reliable PV systems to meet the peak loads of residential neighbourhoods in an optimized manner. (3) Finally, although some studies provide a generalized solution for optimization [17,18], the majority of the methodologies tend to be case and scenario-specific in nature; rendering them irreproducible for other locations/scenarios.

The main objective of this work is to develop and demonstrate an integrated evaluation framework for comparing the feasibility results of CCSPV and DSPV installations for neighbourhood scale. The feasibility analysis includes economic efficiency indicators and technical measures for the performance optimization of components and storage systems for the peak load points. In this regard, this research uses the optimization methods to develop a quantitative optimized model for analysing the opportunities of CCSPV systems to adequately meet the demands of a residential neighbourhood and support the grid. This analysis includes three main metrics that characterize each system type including the level of the energy production in response to the consumption, reliability of the system for peak power and finally the capital cost of implementation for these two systems in residential districts. The proposed solution is reproducible and is not location/scenario specific. The system is designed with minimal constraints and hence, can be modified to suit a particular scenario or location.

The outline of this research is as follows: Section 2 objectively examines the state of art optimization techniques that have been implemented to design PV installations. Section 3 describes the integrated methodology including the process of designing the base case model and then the subsequent design of the PV system components. Section 4 details the pilot case development and the associated results for techno-economic investigations. In this section, different components in the PV system including the PV panel, storage components, and converters are identified and then the optimization process is conducted for CCSPVs and DSPVs. Finally, section 5 discusses the observations and applicability of the integrated methodology in addition to conclusions and suggestions for future work.

2 Literature Review

This section profiles previous research that focuses on energy-sensitive planning strategies for urban neighbourhoods and societies in the context of sustainable cities. Many communities and neighbourhoods plan to implement cost-effective and efficient strategies that leverage renewable energy sources and technologies that are located inside or outside of the area in

question. Other placement options for renewable generation technologies include beyond district boundaries with transmission into the district through energy transactions or within the built environment on brownfield sites or in green spaces [2,19].

PV systems are divided into two categories in terms of their configuration, namely centralized and distributed. In terms of their connectivity, PV systems can be classified as standalone or grid-connected. Also, PV installations can be on-site and off-site based on their location. Centralized PV systems exist as large solar farms as opposed to distributed PV systems that are installed at or near an individual building. Of the two types commonly available, only grid-connected systems can feed electricity directly to the grid. Furthermore, off-site installations are usually grid-connected and centralized while on-site installations can be centralized or distributed and standalone or grid-connected. Figure 1 represents the classification of PV systems.

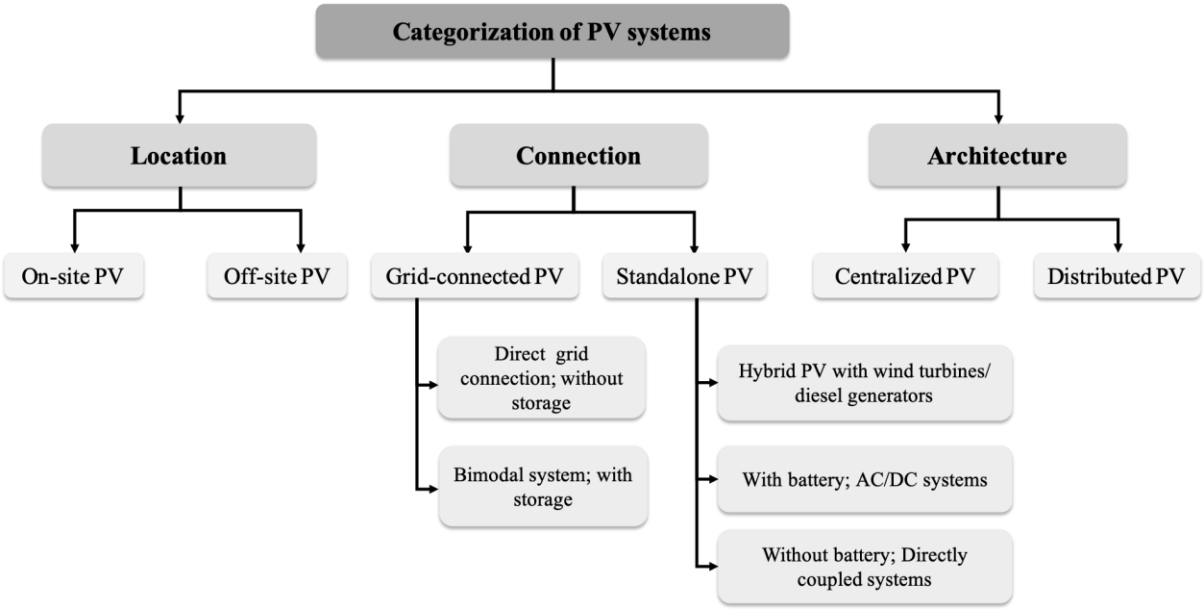

Figure 1- Classification of the different PV systems using: location, system connection and system architecture.

CCSPV panels are gaining popularity as these shared energy generation resources aid in enhancing the access to clean solar energy. The community shared solar systems exist in different architectures, for instance, off-grid centralized, PV storage household systems, grid-connected distributed systems, and PV-battery systems [3]. Augustine (2015) defines community shared solar systems as solar photovoltaic projects that deliver energy and/or economic benefit to multiple customers [20]. Within this system, customers can use their share of the solar PV system without any kinds of physically connected systems to their property

[21]. Community solar business models increase the deployment of solar technology in communities, making it possible for people to invest in solar together [22]. The increasing cost of electricity from the grid can justify using local strategies for market optimization with corresponding reductions in energy costs for urban and rural neighbourhoods [16].

Numerous studies analysed the techno-economic feasibility of different system interactions and identified the effect of such systems on the stakeholders involved. For instance, a study developed a probabilistic model to increase electricity generation and potential investors in community solar by identifying the sources of uncertainties in PV [23]. Another study performed a parametric analysis of PV-battery systems for on-grid locations and concluded that battery installation is mostly price-driven and large PV systems with storage are only viable when selling electricity to the grid [18]. Castillo-Calzadilla et al. determined the differences between three different PV configurations by metrics such as reliability and economic and environmental impacts [24]. The feasibility analysis of these systems demonstrated that DC systems can be used as viable and feasible solutions for energy generation [24]. Barbour et al. (2018) developed a model to balance the energy consumption and generation within a community to determine the potential for community energy storage systems and batteries [25]. Another study examined the interrelationships between PV generation, storage capacity, and on-site consumption to prevent unmanageable load variance and consequent costs [26]. He et al. (2018) employed Homer tool to assess the techno-economic performance of renewable energy-based microgrid scenarios in residential communities in Beijing [27].

A considerable volume of literature relates to PV system optimization which helps in maintaining a balance between investment and operation cost. For optimization of PV electricity generation, three main data categories must be considered including 1) solar irradiation combined with climate data, 2) characteristics of a PV system such as tilt, orientation and shadow impacts, and 3) defining the appropriate time resolutions for recording PV system performance [28]. System optimization ensures power reliability within the system, which is associated with satisfying the load demand requirements. Power reliability is often expressed in terms of load probability that needs to be minimized to achieve a low levelized cost of energy [12].

Different mathematical techniques have been applied for techno-economic optimization of PV panels such as genetic algorithms, linear programming, neural networks, simplex algorithms, and iterative and probabilistic approaches [9]. Khatib (2012) investigated the optimal sizing of

standalone PV systems combined with battery storage systems by proposing two simple equations, which are verified for five test cases in Malaysia [29]. Aghamolaei et al. (2018) implemented an integrated method by using ANOVA and Response Surface Methodology (RSM) to optimize the PV panels' performance in residential neighbourhoods [11]. Another study implemented mixed linear integer programming to explore the possibilities of the influences of potential demand management strategies in overall system cost reduction while presenting a relatively efficient first-pass component sizing for stand-alone micro-grids [15]. Khalilpour (2016) used mixed-integer linear programming to develop a decision support tool for investment decision making, optimal sizing, and operation scheduling of grid-connected PV/battery system with respect to dynamics of periodical weather data, electricity price, PV/battery system cost, PV/battery specifications, desired reliability and other critical design and operational parameters [18]. These studies employ different optimization scenarios, namely, peak shaving potential, renewable energy potential quality, and demand response, with a single objective to identify the size of the PV system. These studies further emphasize the importance of interaction between households and other stakeholders in transitioning to a sustainable power system.

Many studies have addressed the potential of a generation system through optimization methods, however, combined systems with more complicated components are not sufficiently addressed for CCSPV systems. Therefore, an integrated evaluation framework for comparing the feasibility results of CCSPV and DSPV installations at the local scale is presented.

3 Methodology

Because of the fatal triad of carbon emissions, fossil fuel depletion and mounting environmental damage due to the use of oil and coal, cities will have to be powered differently. The use of renewable and distributed micro-power systems is already on the rise today but the current speed of change is much too low to meet global goals in time to avert serious crises. In the context of the research gaps presented, this study presents an integrated quantitative model for analysing the opportunities of CCSPV systems that adequately meet the demands of a residential neighbourhood (Fig. 2).

The process workflow of the methodology is summarized as follows:

- Analysis of the architectural and construction characteristics of buildings to perform energy simulation and identify the consumption profiles.

- Identify the different configurations of PV systems and their associated components suitable for various buildings in the residential block.
- Perform PV size optimizations for identified configurations based on the buildings' consumption profile using grid modelling software.
- Perform a feasibility analysis to associate economic relevance with different PV configurations.

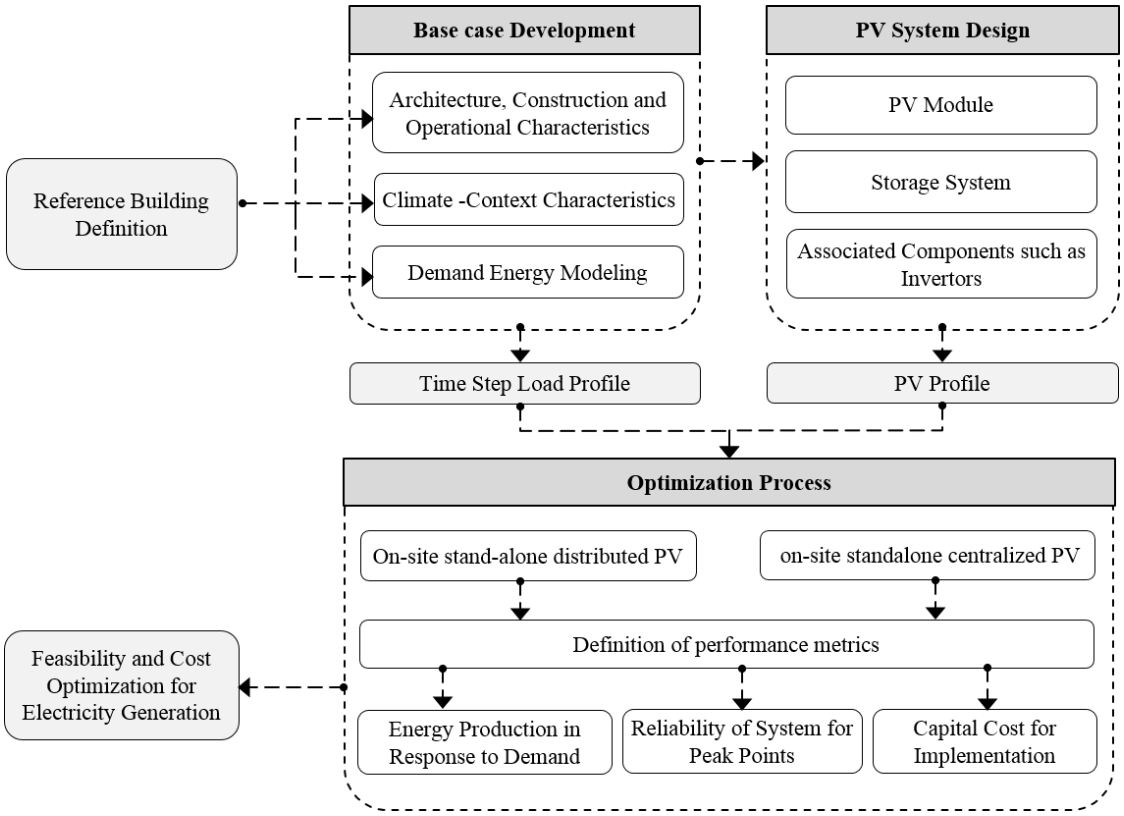

Figure 2- Overall methodology for evaluating the integration of PV systems in neighbourhoods

The methodology investigates the performance of CCSPV and DSPV systems using a base case model. The process of developing the base case is outlined in Section 3.1. Subsequently, the process following the base case development defines the characteristics of PV system components including the PV panel, storage components, and converters, all of which are detailed in Section 3.2. Since component sizing has a significant effect on the performance of the system, the target is to find the optimal size of components for the generation system. Simulation results for each scenario are assessed in Section 3.3 in order to determine the best design alternative based on the characteristics and boundary conditions of each location.

3.1 Base Case Development

The base case development process involves an appropriate representation for the residential block in question. Urban energy modellers often represent a building stock through "building archetypes", i.e. building definitions that represent a group of buildings with similar properties [30]. As the archetype buildings are designated as representative of actual buildings (with data obtained from surveys), the archetypes can be used for modelling the energy demand [30,31]. The archetype approach has been extensively used in the context of national or regional bottom-up building stock models to understand the aggregated impact of energy efficiency policies and new technologies [30,32]. Detailed energy simulations of blocks and neighbourhoods can be performed using the archetype approach even if individual building data is not available for the neighbourhood. It is identified that apartment complexes are usually the most popular dwelling choices for the newly developed blocks of the city.

This process analyses different kinds of residential blocks by using web mapping services, for instance, Google Maps. Such web mapping services enable the analysis and identification of most prominent configurations within the residential building stock. The typical models, considered as residential archetypes, are then mapped into three-dimensional models to generate an overall visualization for their morphological characteristics [31,33]. Three-dimensional modelling software such as SketchUp can be used to import layouts from the web mapping services and develop the models [34]. Further enrichment of these models leverages different libraries consisting of free model assemblies. After the overall understanding of residential configurations using three-dimensional models, the next step is to perform energy modelling with building energy performance simulation tools. The overall process is depicted in Figure 3.

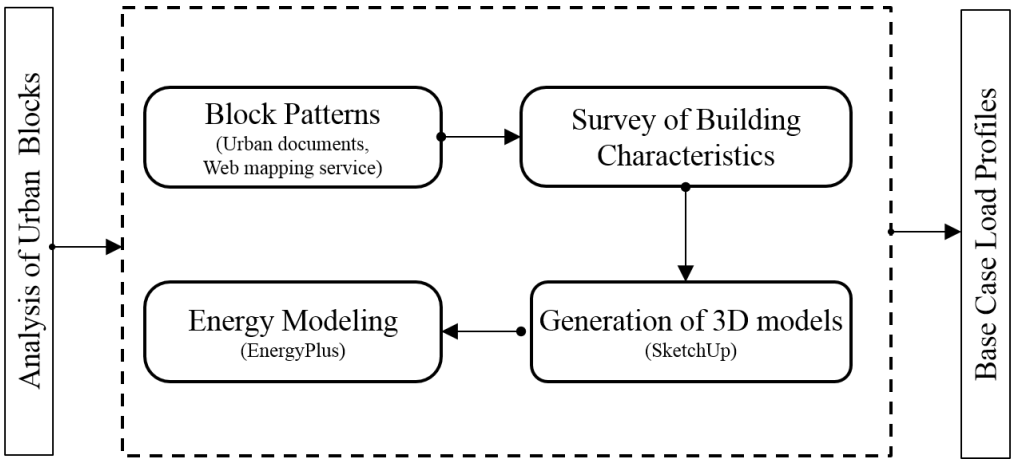

Figure 3-The overall process for modelling building in residential blocks.

These energy models act as reference cases for load profiles of different buildings in blocks. The energy performance modelling is performed in DesignBuilder which makes use of several inputs, for instance, physical parameters, operation schedules etc., to compute the energy consumption associated with different entities [35]. In order to calibrate the building simulation tool and ensure the accuracy of the modelling procedure, the actual energy consumption of buildings was compared with the calculated energy usage. Internal zones are based on the standard zone types in DesignBuilder [35]. The next step is to execute the base case simulation and record the annual energy consumption values by energy subcategory (heating, DHW requirements, lighting and cooling). These consumption profiles are then used as inputs to design the PV system. The design of the PV system mainly involves matching of load demand to the system generation capacity.

The energy modelling is conducted in a subtropical desert/ low latitude arid hot climate. The city of Yazd in Iran is selected for the study. This city has a longitude of 54° 21' E and a latitude of 31° 53' N with an elevation of 1,216 m. Yazd has a subtropical desert/low-latitude arid hot climate with BWh Köppen categorization of hot desert climate. This city is located in the centre of Iran and has considerable solar access with more than 300 sunny days a year. The air temperature in Yazd ranges from -4°C in January to 42°C in July. As demonstrated in Figure. 4, Yazd has significant solar energy potential that can increase the potential for renewable electricity generation.

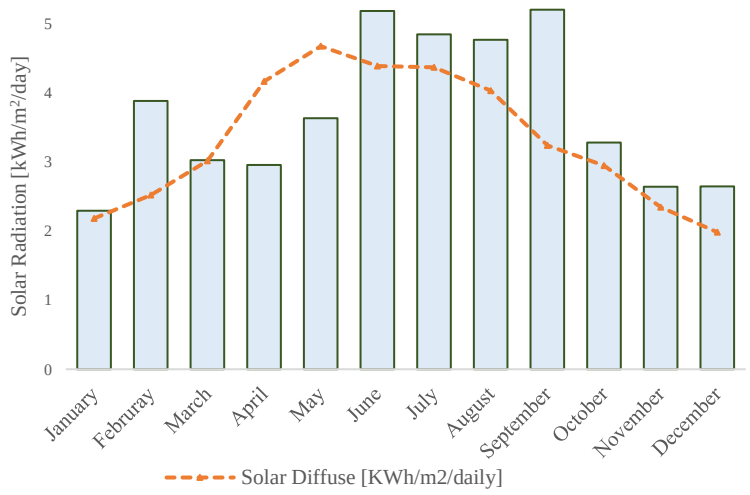

Figure 4-Average solar potential for direct and diffuse solar radiation in Yazd based on hourly weather data

To calculate the energy consumption of this residential block, electricity and gas loads of heating, cooling and lighting systems are determined. The heating and cooling system,

occupancy schedules, activity pattern in each zone, setpoint settings and construction characteristics have been modelled in according to the detailed survey of characteristics and available documents and are assumed to be the same over the analysis period [36–39]. The building's heating systems comprise gas boilers (with a heating CoP of 0.85) that deliver hot water to radiators located in the interior spaces. The cooling systems employ chillers that are integrated with fan coils (with a cooling CoP of 1.80). These two systems represent typical HVAC systems used in tall residential buildings of Iran [36–38]. The heating and cooling setpoints are defined as 22°C and 28°C respectively. The occupancy schedules of this residential building (heating system: October to February and cooling system: June to September) and activity for each zone are modelled in detail according to the surveyed features of that building and are assumed to be consistent during the analysis. Electrical loads are assumed for a variety of minor and major appliances, lighting systems and cooling systems.

The approach considers LED lighting systems for residential blocks as is a common installation for these apartment buildings [36–39]. The construction profile of buildings is defined as follows; the infiltration rate of each building is set to 0.7 ach which shows airtightness of apartments. The U-Value for the windows performance is 1.9 W/m^2-K while the U-value for external walls is set to 0.35 W/m^2-K. The effective inputs for energy modelling are presented in Table 1.

Table 1- The initial settings for running the simulation

Category	Inputs	Value	Ref
Time of simulation	Time of simulation	Annual (2017)	
	Time interval	Hourly based	
Location	City	Yazd, Iran	
	Location on the earth	Longitude: 54° 21' E, Latitude: 31° 53' N	[11,38,40]
	Elevation	1,216 m	
Climate	Condition	Subtropical desert/low-latitude arid hot climate	
	Type	BWh Köppen category	
	Average air temperature	Min: -4°C (January), Max: 42°C (July)	
	Average relative Humidity	Min:15% (July), Max: 51% (January)	[38,40,41]
	Solar radiation (Direct Normal Irradiation (DNI))	Max: 5253 Wh/m² (September)	
	Sunny days in a year	More than 300 days	
Construction	Infiltration rate	0.7 ACH	
	U-Value of the Glazing	1.9 W/m^2-K	
	U-value for external walls	0.35 W/m^2-K	
	Roof U-Value	0.6 W/m^2-K	
Cooling system	Type	Chiller with fan coils	
	CoP	1.80	[36–39]
	Occupation	June to September	
	Set point	28°C	
Heating system	Type	Gas boiler with standard radiators	
	CoP	0.85	
	Occupation	October to February	
	Set point	22°C	

3.2 PV system design

Sizing of the PV array and battery bank for a SPV system is an important part of system design, which in turn requires the data on solar radiation and load demand. There are three basic ways of integrating PV systems in buildings, namely, roof-based systems, facade systems and sunshades and sunscreens. These systems are designed in a way to avoid additional constraints (such as appearance or airtightness) on the buildings. This study mainly focuses on roof-based PV panels as these systems are often free from over shading and roof slope can be selected to boost PV performance. Furthermore, from functional and aesthetic perspectives, it may be easier to integrate PV systems onto a roof. This electricity can be used at night by employing a storage mechanism. Batteries used for this purpose must have a large storage capacity [42]. A typical PV system contains PV panels, converter and batteries. The details of the selected system for this study are included in Appendix B.

A PV panel is often characterized by the total power generated, which can be calculated using (1).

$$P_{PV} = n_{PV} V_{PV} i_{PV} \tag{1}$$

Where n_{PV} denotes the number of PV panels, V_{PV} and i_{PV} are the voltage and current of the PV panel. To account for various physical and environmental interactions, the output of a PV panel is usually calculated using (1a).

$$P_{pv} = \frac{f_{pv} Y_{PV}\, I_T}{I_s} \tag{1a}$$

where f_{PV} is the PV derating factor and accounts for the effects of dust on the panel, wire losses, or elevated temperature that would cause the output of PV array to deviate from the ideal conditions. Y_{PV} (kW) is the rated capacity of the array. I_T (kW/m^2) is the global solar radiation incident on the surface of PV array, and I_S is 1kW/m^2, which is the standard amount of radiation used to rate the capacity of PV array.

The optimum operating point current and voltage of a PV panel are calculated using (2) and (3).

$$i_{PV} = i_{SC}\left(1 - C_1\left[\exp\left(\frac{V_{PV} - \Delta V}{C_2 V_{OC}}\right) - 1\right]\right) + \Delta i \tag{2}$$

And

$$V_{PV} = V_{mp}\left(1 + 0.0539 \log\left(\frac{I_T}{I_{st}}\right)\right) + \beta_0 \Delta T \tag{3}$$

Where

$$C_1 = \left(1 - \frac{i_{mp}}{i_{SC}}\right) \exp\left(-\frac{V_{mp}}{C_2 V_{OC}}\right) \quad (4)$$

$$C_2 = \frac{V_{mp}}{(V_{OC} - 1) \ln\left(1 - \frac{i_{mp}}{i_{SC}}\right)} \quad (5)$$

$$\Delta V = V_{PV} - V_{MP} \quad (6)$$

$$\Delta i = \alpha_o \left(\frac{I_T}{I_{st}}\right) \Delta T + \left(\frac{I_T}{I_{st}} - 1\right) i_{SC} \quad (7)$$

$$\Delta T = T_{cell} - T_{st} \quad (8)$$

$$T_{cell} = T_A + 0.02 I_T \quad (9)$$

Where i_{PV} is the optimum operating point current of the PV panel and V_{PV} is the optimum operating point voltage of the PV panel. i_{SC} is the short-circuit current, V_{mp} and i_{mp} are the maximum power voltage and current, V_{OC} is the open-circuit voltage, α_o is the current temperature coefficient and β_o is the voltage temperature coefficient of the panel. T_{cell} is the temperature of the PV cell. C_1 and C_2 are two constants calculated using eq. (4) and eq. (5). ΔV, Δi and ΔT represent the differential voltage, current and temperature and are calculated using eq. (6), eq. (7) and eq. (8) respectively. I_T is the total solar irradiance on tilted panel, I_{st} is the standard solar irradiance (1000 W/m^2) and T_A is the ambient temperature [37]. The standard ambient temperature is T_{st} = 25^{0}C. Commercially available PV simulation software makes use of Eqs. (1-9) to model the PV.

Energy supply systems based on renewable energy sources require energy storage because of their fluctuation and the insufficient certainty of supply. Due to the stochastic nature of the electrical output of PV systems, energy storage is needed to supply the load “on demand” by storing energy during periods of high irradiance [43]. There are different kinds of batteries that have been used as a storage bank in photovoltaic applications. Most popular ones in these applications are Lithium-ion batteries, which outperform other batteries in energy and power

densities and round trip efficiency [44]. These batteries are also characterized by their long cycle life leading to reduced life-cycle costs [45].

Batteries are modelled based on their charging and discharging cycles. The number of life-cycles reduces with the Depth of Discharge (DOD) [46]. Also, a few models use the current-voltage characteristics of a battery as a function of State of Charge (SOC) [47]. During the charging mode (output from the PV panels is greater than the demand), the available capacity of the battery is a function of time and can be expressed as in Eq. (10).

$$C(t) = C(t-1).(1-\sigma) + \left(P_T(t) - \frac{P_L(t)}{\eta_{conv}}\right)\eta_{Batt} \tag{10}$$

Where P_T is the total output power generated by the system, P_L is the load at the corresponding hour, η_{conv} is the efficiency of the converter, η_{Batt} is the charging efficiency and σ is the self-discharge rate of the battery.

During the discharging mode, the battery capacity can be expressed as in Eq. (11).

$$C(t) = C(t-1).(1-\sigma) + \left(\frac{P_L(t)}{\eta_{conv}} - P_T(t)\right)\eta_{Batt} \tag{11}$$

The charge capacity of the battery storage must always be maintained within the limits. The maximum limit is the nominal capacity of the battery while the minimum is determined by the maximum DOD (normally 80%).

A converter is required for a system in which DC components serve as an AC load or vice versa. It can operate as a rectifier which converts AC to DC, an inverter which converts DC to AC, or both.

3.3 System optimization

This process enables identification of the optimal size for each of the components in the PV system. Besides, this process also aids in the identification of overall system size for centralized and distributed installations required to support a similar load. For each time step, the electric and thermal demand in that time step is compared to the energy that the system can supply and the flow of energy to and from each component of the system is calculated. For systems that include batteries or fuel-powered generators, how to operate the generators and whether to charge or discharge the batteries is also determined in each time step. Component size optimization is performed by either fixing various sizes of the components or by specifying the lower and upper limits of the component size range. It is possible to specify the maximum number of simulations per optimization, system design precision, and Net Present Cost (NPC)

precision and focus factor. The maximum number of simulations per optimization prevents the optimization from running indefinitely if convergence cannot be achieved. The system design precision specifies the relative error in the decision variables (i.e., PV array capacity) below which convergence is allowed.

This study performs these energy balance calculations for each system configuration and determines whether a configuration is feasible. The process subsequently estimates the cost of installing and operating the system over the lifetime of the project. System financial calculations account for costs that include capital, replacement, operation and maintenance, fuel, and interest.

4 Results

This section describes the implementation of the devised methodology and shows the results for the selected case.

4.1 Base case identification results

To ensure the accuracy of the research, a model that is a representative of the most prominent residential block is chosen based on various configurations of existing blocks. Here, blocks are defined by focusing on spatial aspects including two main factors of network design and similarity of architecture style of buildings in each block [48,49]. Therefore, from the web mapping process and reviewing the master plans of the city, it was identified that apartment complexes are usually the preferred and prominent dwelling choice for the newly developed blocks of the city [31,38,50]. Also, apartment complexes usually provide a larger inhabitant to area ratio, which is necessary to cater to the housing needs of a growing population.

Hence, apartment complexes as a representative of the new developments in the city are selected for the reference case of this study. A residential block comprising ten similar apartment complexes is chosen as the reference case for the energy modelling process. The block is located in the outskirts of the city and, each apartment complex in the block consists of 9 storeys. These 10 buildings are characterized on the basis of peak power consumption.

The next step after choosing the base case model is to execute the energy simulation to generate annual consumption profiles. In this regard, the hourly weather data is used to analyse the consumption and solar radiation for a complete year [40]. Although the 10 building complexes of this block are similar to each other, the results of energy consumption differ due to different reasons such as the orientation of buildings [51,52]. Results of energy simulations for these 10

buildings show that these buildings can be categorized into four archetypes with similar energy performance results. Here, the energy performance of one of these apartment buildings broken down by energy usage subcategory (heating, DHW requirements, lighting and cooling) is shown as a sample in Figure 5. Moreover, the energy consumption results of the other three apartments in Appendix A.

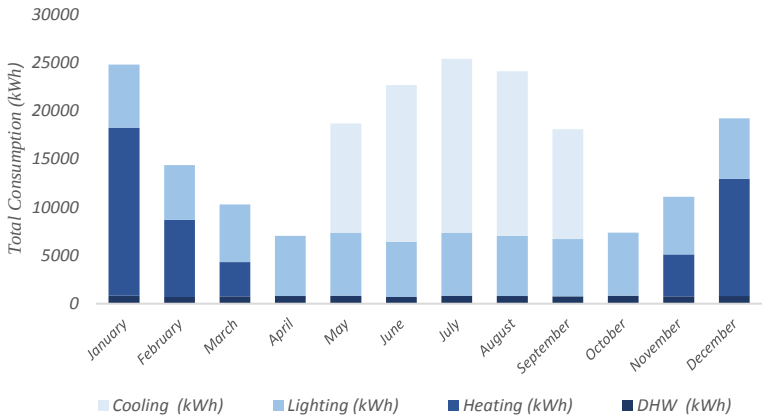

Figure 5- Monthly energy consumption profile for one of the apartment buildings in the residential block. The figure identifies the major end uses with heating dominating during winter and cooling dominating during summer. Lighting and DHW remain relatively constant throughout the year.

As the peak loads have occurred in the cooling profiles, we designed the PV systems to meet the cooling loads of these four archetypes. Moreover, the cooling demand represents the highest hourly peak amongst all the other end uses. Therefore, the PV system designed to match the cooling load will also satisfy the heating. The day chosen for the analysis is 3rd August, the standard cooling design day at 99% design temperature for Yazd.

The PV system is designed to match the maximum system of these four archetypes. The results show that there are four distinct hourly cooling load profiles (Fig. 6). Maximum peak cooling load in the cluster of ten building is 253 kW_p, as depicted in Fig. 6(a). There are two buildings in the neighbourhood that belong to this category. The peak cooling loads of the remaining three profiles are relatively close to each other. The second maximum peak cooling load is 94.31 kW_p, shown in Fig. 6(b) and two buildings in the neighbourhood fall into this category. Five buildings in the neighbourhood belong in the category of 83.31 kW_p peak cooling load, depicted in Fig. 6(c). There is only one building that falls into the last category of 78.60 kW_p peak cooling load, as shown in Fig. 6(d).

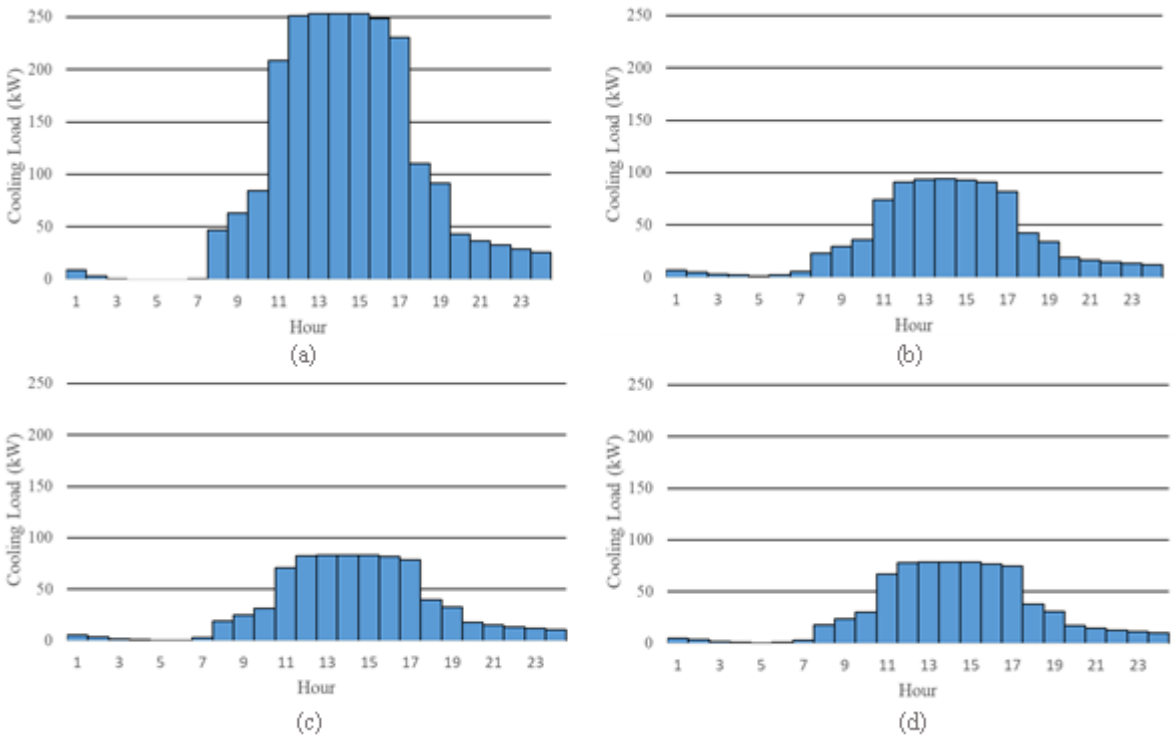

Figure 6- Cooling load profiles of buildings in the neighbourhood. (a) Building with 253.39 kW peak cooling load. (b) Building with 94.31 kW peak cooling load (c) Building with 83.31 kW peak cooling load (d) Building with 78.60 kW peak cooling load.

4.2 Technical Analysis: Identification and Optimization

The PV system size is calculated by running optimization routines. The hourly cooling consumption profile is fed into HOMER, which then optimizes the system based on the least cost and identifies the optimum result. These apartment buildings provide considerable roof area for PV panel installation including 450 to 530 m^2 for each building. Satellite photos and location maps indicate that the area does not have trees or other types of shadings around these apartment complexes affecting the PV performance. Furthermore, there is no obstruction due to shading from the individual buildings (Appendix A: Figure 12).

The priority is to cover the loads based on the hourly time series. The next filter is to sort results by their cost which includes the capital cost, operation and maintenance costs. The optimization process applies two in-built algorithms: 1) the original grid search and 2) a proprietary derivative-free algorithm, to calculate the economic and technical feasibility of different scenarios. The original grid search algorithm simulates all of the feasible system configurations defined by the search space. The proprietary derivative-free algorithm searches for the least-

cost system. These algorithms significantly simplify the design process for identifying the least-cost options for micro grids or other distributed generation electrical power systems [53].

The inputs to the model include cooling demand profiles of buildings in the block, energy resources to generate electricity and storage battery to ensure efficient energy use. The system is defined based on the above inputs along with optimized sizing of each piece of equipment, which is then coupled with economic analysis based on the NPC, NPV and cash flow of the system (Fig. 7).

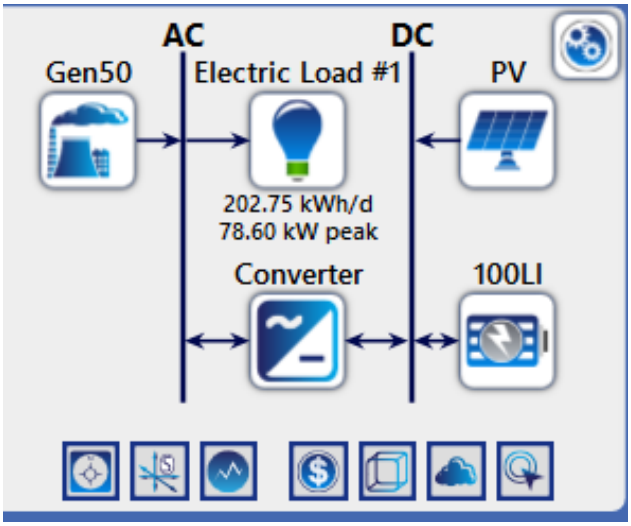

Figure 7- Overall system as implemented in HOMER. The system consists of a generator acting as the system base, PV panels, Lithium-ion batteries, electric loads and a converter.

PV systems are only optimized based on load profiles to identify scenarios and opportunities for distributed and centralized PV installations at a neighbourhood scale. Furthermore, we have optimized the PV systems based on different levels of PV penetration and hence, in the event of unavailability of roof area for distributed installations, PV penetration at the building level can be reduced accordingly. To conduct the feasibility analysis, a DSPV system is assumed for each individual building and a simulation is run to identify the system size along with other desired system components, tabulated in Table 2. The results are then compared to the case where a single centralized SPV system is considered for the neighbourhood, as tabulated in Table 3. Different PV penetration levels are analysed to ensure the consistency of results.

Identification of the number of panels involves the use of PV system size. For instance, PV system size (802kW; Table 2) is used to identify the number of panels required for a peak load of 253.39kW. There are different combinations possible to attain the system requirements. For instance, the 802kW (~800kW) PV system can be divided into two subsystems of 400kW each.

Each 400kW subsystem can be further divided into four substations of 100kW equipped with an inverter. Hence, considering each single PV system of 4kW,

$$Total\ number\ of\ PV\ systems\ per\ 100kW\ branch = \frac{Total\ branch\ power\ capacity}{PV\ system\ capacity}$$

$$Total\ number\ of\ PV\ systems\ per\ 100kW\ branch = \frac{100kW}{4kW} = 25$$

Similarly,

$$Total\ number\ of\ PV\ sytems\ in\ 400kW\ subsytem = 25 * 4 = 100$$

$$Total\ number\ of\ PV\ sytems\ required = 100 * 2 = 200$$

Hence, a PV system of 802kW requires 200 PV systems of 4kW each. It is worthwhile to note that different combinations of branches and subsystems are possible. The combinations vary on the basis of inverter and PV panel specifications.

Table 2- Sizing of the different system components considering DSPV installation for varying levels of PV penetration.

Case Number	Peak Load (kW)	System Base (kW)	PV Penetration (%)	Optimized PV System Size (kW)	Converter Size (kW)	Number of 100 kWh Li-Ion batteries	Annual PV Electricity Production (kWh)
Case 1	253.39	0	100	802	264	10	1,424,438
		150	71	269	204	2	477,901
		200	37	115	88	1	204,430
Case 2	94.31	0	100	258	129	6	457,928
		50	71	105	84	1	186,489
		60	37	52.6	49.9	1	96,633
Case 3	83.31	0	100	274	96.9	4	486,242
		30	71	95.9	55.3	5	170,270
		50	37	37.1	34.7	1	65,900
Case 4	78.60	0	100	254	87.4	4	450,549
		35	71	83.5	50.4	4	148,231
		55	37	32.6	29.3	1	57,866
Total	1190.5	0	100	3998	1358	56	6,646,941
		550	71	1311	903	30	2,328,361
		800	37	501	479	10	989,512

Table 3- Sizing of different system components considering a CCSPV installation for varying levels of PV penetration.

Peak Neighbourhood Cooling Load (kW)	System Base (kW)	PV Penetration (%)	Optimized PV System Size (kW)	Converter Size (kW)	Number of 100 kWh Li-Ion batteries	Annual PV Electricity Production (kWh)
1190.5	0	100	3690	1310	48	6,554,808
	550	71	1259	806	15	2,600,386
	800	37	400	306	8	1,063,582

4.2.1 PV system components

As evident from the results, the PV system size reduces by a considerable amount when a CCSPV system is considered for the neighbourhood. For instance, considering the case of 100% PV penetration level, the optimized system size of a centralized SPV architecture to support the total peak load of 1190.5 kWp would be 3690 kW. If a distributed PV architecture is assumed for the neighbourhood, it would require around 3998 kW of PV installation to support the same peak load although now distributed over 10 buildings using individual PV panels. Table 4 lists the comparison results for DSPVs and CCSPV. For each penetration level, the combined size of the DSPV installation is found to be greater than the centralized SPVs. This relates to the fact that a centralized SPV installation is more efficient and economical in terms of overall system size than DSPV installation.

Table 4- Comparison of the system size for CCSPV and DSPV installations.

PV Penetration (%)	Optimized PV System Size (kW)		Converter Size (kW)		Number of 100 kWh Li-Ion batteries	
	CCSPV	DSPV	CCSPV	DSPV	CCSPV	DSPV
100	3690	3998	1310	1358	48	56
71	1259	1311	806	903	15	30
37	400	501	306	479	8	10

4.2.2 Storage system

To use the system in an efficient manner, storage systems are evaluated in the neighbourhood. Battery sizing analysis is performed to determine the optimal size and number of batteries. 100 kWh Lithium-ion batteries (optimal size) are considered with the CCSPV and DSPV. From Table 4, it is evident that the number of batteries required for centralized SPVs is always less than for DSPVs for the entire range of penetration levels. It can be attributed to the fact that for

a centralized SPV system, the surplus energy generated from the PV panels can be always utilized within the network or stored in a battery. However, for a DSPV installation, the surplus energy can only be stored in batteries with incompatible capacities. This observation highlights the importance of interlinking that exists in the centralized architecture, thus optimizing the energy flow across the buildings in the neighbourhood.

4.2.3 Converter size

The variations in the converter size follow a similar pattern as for the PV system size. Owing to the fact that the PV system size is less for the centralized installation, the converter size required to serve that installation is also less. Again, from Table 4, it can be concluded that the converter sizes for different penetration levels are smaller for centralized SPV architectures than for the distributed ones. Hence, CCSPV installation results in a system which is more efficient and economically viable.

4.3 Economic analysis

The economic efficiency is one of the main concerns of investors and stakeholders in PV projects. This is due to the fact that the results of economic feasibility guarantee the implementation of the project in different stages and encourage the investors to fund other similar projects.

The economic performance of the CCSPV and DSPV configurations is evaluated using the NPC, NPV and cash flow parameters. The actual data for fuel price and electricity production is taken from the real-time pricing data [54]. The NPC of a component is the present value of all the costs of installing and operating the component over the project lifetime, minus the present value of all the revenues that it earns over the project lifetime. The total NPC is obtained by summing the total discounted cash flows in each year of the project lifetime. Costs include capital costs, replacement costs, Operation and Maintenance (O&M) costs, and fuel costs. The capital cost of a component is the total installed cost of that component at the beginning of the project. O&M cost of a component is the cost associated with operating and maintaining that component. The total O&M cost of the system is the sum of the O&M costs of each system component. The fuel cost is the annual cost of fueling the generator. Salvage value is the value remaining in a component of the power system at the end of the project lifetime. The project lifetime is the length of time over which the costs of the system occur. The real discount rate is used to convert between one-time costs and annualized costs. NPV estimates the current value of the project assuming a fixed price of electricity (0.21 USD/kWh).

In this step, the economic analysis is performed to present the feasibility of each system based on economic priorities. Figure 8 includes the NPC for DSPV configuration for different levels of PV penetration. The cost breakdown for the CCSPV configuration is in illustrated in Figure 9.

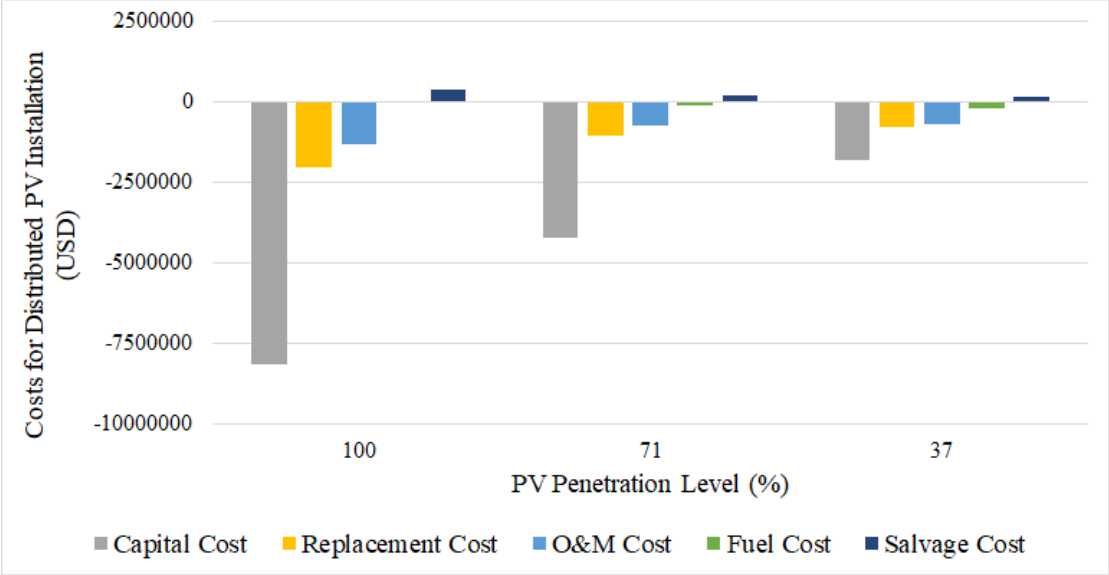

Figure 8- Cost Breakdown for DSPV for different PV penetration levels (total). The individual costs include capital cost, replacement cost, O&M cost, fuel cost and, salvage cost.

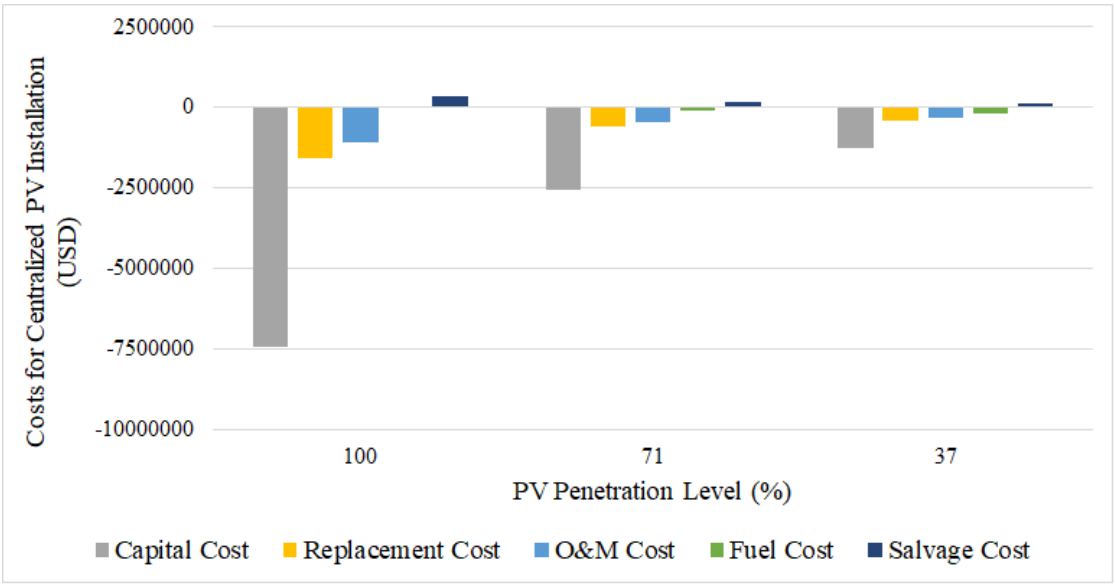

Figure 9- Cost Breakdown for CCSPVs for different PV penetration. The individual costs include capital cost, replacement cost, O&M cost, fuel cost and, salvage cost.

Figure 10 presents the comparison of NPCs for DSPVs and CCSVs. CCSPVs are economically more viable than DSPVs. For PV penetration levels of 71% and 37%, savings are almost 35% when installing CCSPV.

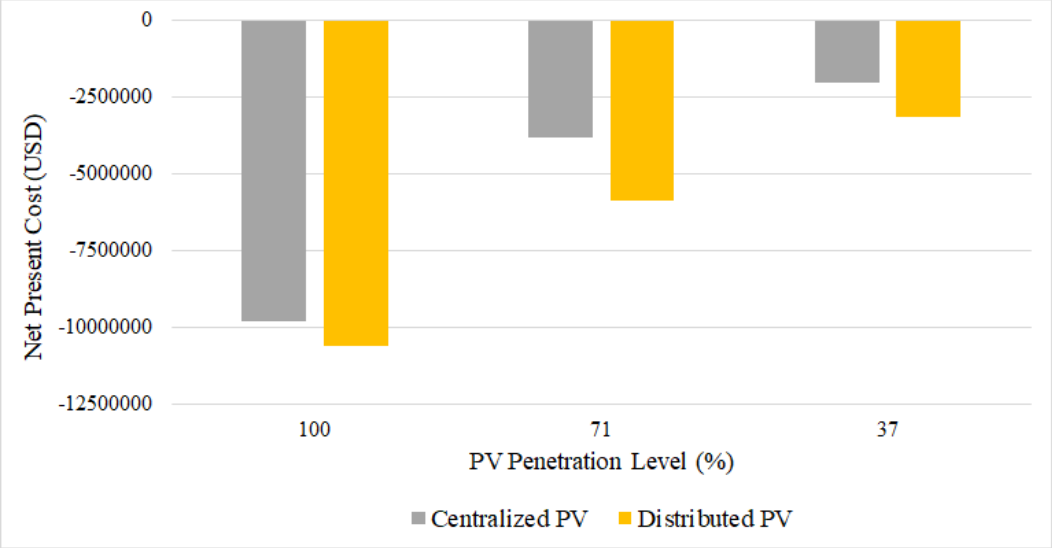

Figure 10- Comparison of NPCs for CCSPV and DSPV installations. All the negative values depict negative cash flows.

Furthermore, CCSPV installations result in positive NPVs for all levels of PV penetration while DSPV installations result in negative NPVs for lower levels of PV penetration (Figure 11).

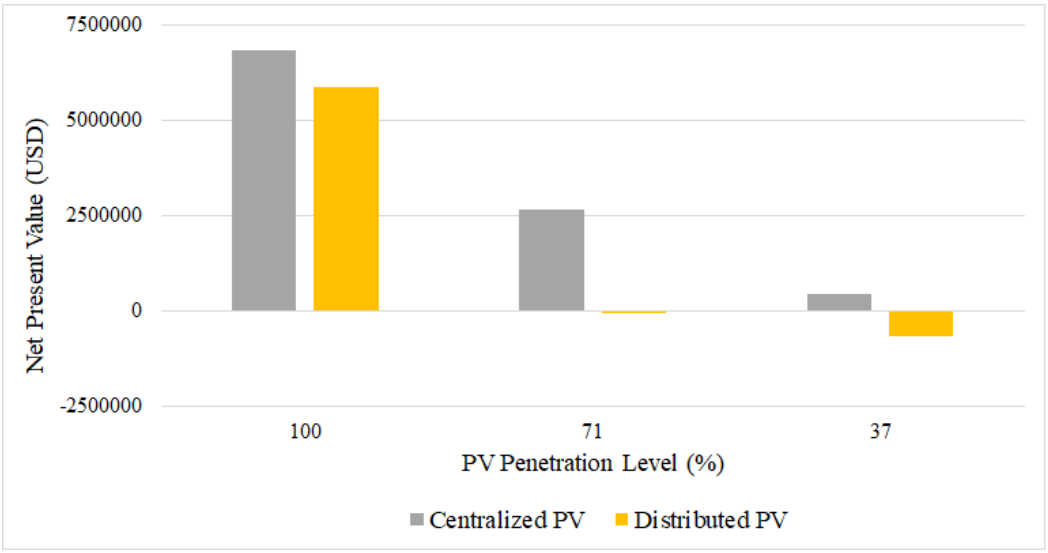

Figure 11- Comparison of NPVs for CCSPV and DSPV installations. Positive values depict positive cash flows and negative values depict negative cash flows.

5 Discussion

Zero energy districts are viable solutions towards balancing the annual energy demand using electricity generated from renewable energy sources [2]. The studies conducted in the literature considered centralized installations to be suitable only as grid stand-alone systems [55]. Also, DSPV installations are often the preferred choice for urban city planners when planning new

neighbourhoods [56]. However, with a shift towards renewable energy and smart cities, centralized SPVs would prove to be more beneficial, having established that these installations perform better in terms of overall efficiency and meet a higher proportion of occupant energy demands [57]. Although the literature on the techno-economic analysis of PV panels has experienced a major boost in the last decade, not many studies have focused on the feasibility analysis of community-based and local centralized PV systems at a residential neighbourhood scale.

In this research, the techno-economic analysis of CCSPV system was discussed. Technical analysis includes three metrics of PV components definition, storage systems, and converter size. Regarding the PV component overall size, comparing the results for DSPV and CCSPV architectures demonstrates that in different PV penetration rates, the CCSPV system requires smaller size. Considering the case of 100% PV penetration level, the optimized system size of a CCSPV architecture to support the total peak load of 1190.5 kW_p would be 3690 kW. If a DSPV architecture is assumed for the neighbourhood, it would require around 3998 kW of PV installation to support the same peak load although now distributed over 10 buildings using individual PV panels (Table 4). By reducing the penetration level to 71%, the requirement of PV system is about 1259 kW for the centralized system while the distributed installation requires 1311 kW. This difference would be more significant when the penetration level is lower, for instance, the PV components' overall size would be lower by about 25% when implementing the centralized system at the neighbourhood scale (Table 4).

To use the system in an efficient manner, storage systems are also evaluated in the neighbourhood. By considering the same Lithium-ion batteries, centralized and DSPVs require a different number of batteries which is always lower for the CCSPVs. For 71% penetration level of PV generation, the required batteries for centralized panels are 50% lower when compared to the distributed system. This feature significantly contributes to the economic efficiency of PV storage systems [18].

The performance pattern of the converter size follows a similar pattern as for the PV system size. The converter size varies considerably to respond to the PV systems in peak load points. The variation pattern is more vibrant for lower levels of PV penetration. For instance, at the level of 100% PV penetration, the converter requirement of the system is about 1310 kW for CCSPV system while it is increased to 1358 kW when implementing the distributed architecture. However, by reducing the penetration level to 37%, the system requirement is

dropped to 35% in a centralized architecture. Hence, CCSPV results in a system which is more efficient and economically viable.

This system resulted in a decrease in the size of the PV system, the required converter size and a number of batteries needed to store the surplus energy. This is due to the fact that increased interactions of energy flow between different buildings in the neighbourhood facilitate the optimized use of available resources. Moreover, transmission losses are reduced and multiple connections are available, usually at a higher voltage level. Furthermore, the presence of a manageable number of inverters results in relatively straight forward monitoring and easy access to individual central inverters.

The economic efficiency is a promising factor to encourage investors to implement PV system in different spatial scales from individual buildings to community scales or solar farms. The economic performance of the CCSPV and DSPV configurations is evaluated using NPC parameter which includes capital costs, replacement costs, O&M costs, NPV and fuel costs. For PV penetration level of 100%, centralized installations are 7% cheaper than the distributed installations. For PV penetration levels of 71% and 37%, savings are almost 35% when installing centralized PV plants (Figure 10). These benefits enable affordable and efficient PV installations for a neighbourhood. CCSPV installations result in positive NPVs for all levels of PV penetration while DSPV installations result in negative NPVs for lower levels of PV penetration (Figure 11). Centralized installations offer a maximum level of efficiency with low self-consumption, thus, enabling the highest possible yields.

CCSPVs, although capital intensive, have been receiving enhanced investments as opposed to DSPVs. Most of the countries currently subsidize renewable power producers with billions of euros a year, regardless of demand. Because network development lags far behind, a lot of power is wasted. With CCSPVs, the grid would be able to achieve two objectives single-handedly; (1) empower the customers, and (2) achieve an indirect control over micro-grids.

The results of this study confirm that for implementing PV systems in residential neighbourhoods and communities of this climate, it is necessary to receive financial support from the government to reduce the rate of NPC and O&M costs. As results show the economic performance of PV panels for both presented systems cannot highly encourage consumers of fossil fuel electricity to install these new systems (Figures 8 &9). However, these systems can be quite economically feasible by receiving governmental supports. As governmental financial support can play a prominent role in the development of these systems since without adopting such strategies, the high initial costs of PV panels discourage private investors to replace

electricity from fossil fuels with clean electricity [9]. Studies have shown that deployment policies have been established all over the world which resulted in positive growth in annual installation from 2.67 GW in 2007 to 37.6 GW in 2013 [9].

6 Conclusion

This research investigated the importance of CCSPV systems as opposed to the already established DSPVs. The feasibility analysis includes economic efficiency indicators and technical measures for optimizing the performance of components and storage systems for the peak load points. This analysis incorporates three main metrics including the level of the energy production in response to the consumption, reliability of the system for peak power and finally the capital cost of implementation. The economic analysis is evaluated using NPC parameter which includes capital costs, replacement costs, O&M costs, NPV and fuel costs.

Results revealed that CCSPVs perform more efficiently than DSPVs in terms of overall system size and economic analysis. CCSPVs offer a maximum level of efficiency with low self-consumption, thus, enabling the highest possible yields. Regarding the PV component overall size, the CCSPV resulted in a decrease in the size of the PV system, the required converter size and a number of batteries needed to store the surplus energy. Regarding the economic performance, CCSPV installations result in positive NPVs for all levels of PV penetration while DSPV installations result in negative NPVs for lower levels of PV penetration.

As there has been an emerging trend to transform the entities of the built environment to become an active part of the energy system, CCSPVs will allow buildings to play an active role in managing the flow of energy. Such installations will allow a reduction of peak utility loads and with the advent of new tracking systems, the peak PV output could be increased across the whole day. A centralized PV installation would ensure optimization of the PV system size and of the components attached to the system.

Besides the aforementioned potentials of PV systems in neighbourhood scale, there is no single choice that results in an optimal PV system concept; instead, a wide range of technical and commercial requirements must be weighed in combination with the client's highly individual needs. An important restriction of implementing community-based PV systems is that these systems require huge vacant public spaces. Provision of such spaces increases the initial costs of the project. Moreover, another important issue of CCSPV is the possibility of decreasing the aesthetic values of the neighbourhood or causing discomforts such as glare of sunlight for vehicle drivers and pedestrians.

Although the results establish the benefit of considering CCSPVs for neighbourhoods, there are certain aspects that have not been taken into account. Buildings' features such as form, transparency ratio of facade and orientation and also climatic features of the context and location of each study considerably impact on the results of feasibility analysis. As the characteristics of different locations have a huge impact on the results of feasibility analysis, further studies can investigate the application of the suggested feasibility framework in other climate contexts and provide comparative analysis between their results.

Acknowledgement

This publication has emanated from research conducted with the financial support of Science Foundation Ireland under the SFI Strategic Partnership Programme Grant Number SFI/15/SPP/E3125'.

7 References

[1] United Nations, World Urbanization Prospects The 2007 Revision Highlights, 2007.

[2] R. Aghamolaei, M.H. Shamsi, M. Tahsildoost, J. O'Donnell, Review of district-scale energy performance analysis: Outlooks towards holistic urban frameworks, Sustain. Cities Soc. 41 (2018) 252–264. https://doi.org/10.1016/j.scs.2018.05.048.

[3] T. Castillo-Calzadilla, A.M. Macarulla, O. Kamara-Esteban, C.E. Borges, Analysis and assessment of an off-grid services building through the usage of a DC photovoltaic microgrid, Sustain. Cities Soc. 38 (2018) 405–419. https://doi.org/10.1016/j.scs.2018.01.010.

[4] C.L. Choguill, Developing sustainable neighbourhoods, Habitat Int. 32 (2008) 41–48.

[5] P.A. Torcellini, D.B. Crawley, Understanding zero-energy buildings, ASHRAE J. 48 (2006) 62.

[6] T. Martins, L. Adolphe, L. Bastos, From solar constraints to urban design opportunities: Optimization of built form typologies in a Brazilian tropical city, Energy Build. 76 (2014) 43–56. https://doi.org/10.1016/j.enbuild.2014.02.056.

[7] L.W.A. van Hove, C.M.J. Jacobs, B.G. Heusinkveld, J.A. Elbers, B.L. van Driel, A.A.M. Holtslag, Temporal and spatial variability of urban heat island and thermal comfort within the Rotterdam agglomeration, Build. Environ. 83 (2015) 91–103. https://doi.org/10.1016/j.buildenv.2014.08.029.

[8] R. Uther, R. Zilles, Making the case for grid-connected photovoltaics in Brazil, Energy Policy. 39 (2011) 1027–1030. https://doi.org/10.1016/j.enpol.2010.12.021.

[9] X. Zhang, M. Li, Y. Ge, G. Li, Techno-economic feasibility analysis of solar photovoltaic power generation for buildings, Appl. Therm. Eng. 108 (2016) 1362–1371. https://doi.org/10.1016/j.applthermaleng.2016.07.199.

[10] T. Castillo-Calzadilla, A.M. Macarulla, O. Kamara-Esteban, C.E. Borges, Feasibility and simulation of a solar photovoltaic installation in DC for a standalone services building, DYNA Ing. E Ind. 93 (2018) 24–30. https://doi.org/10.6036/8410.

[11] R. Aghamolaei, M.R. Ghaani, M. Tahsildoost, M. Zandi, A comprehensive energy-oriented approach for optimization of solar potential in urban contexts: an application study for residential districts, Adv. Build. Energy Res. 13 (2019) 205–219. https://doi.org/10.1080/17512549.2018.1488613.

[12] D. Saheb-Koussa, M. Haddadi, M. Belhamel, Economic and technical study of a hybrid system (wind–photovoltaic–diesel) for rural electrification in Algeria, Appl. Energy. 86 (2009) 1024–1030. https://doi.org/10.1016/j.apenergy.2008.10.015.

[13] D.P. Kaundinya, P. Balachandra, N.H. Ravindranath, Grid-connected versus stand-alone energy

systems for decentralized power-A review of literature, Renew. Sustain. Energy Rev. 13 (2009) 2041–2050. https://doi.org/10.1016/j.rser.2009.02.002.

[14] A. Chaurey, T.C. Kandpal, Assessment and evaluation of PV based decentralized rural electrification: An overview, Renew. Sustain. Energy Rev. 14 (2010) 2266–2278. https://doi.org/10.1016/j.rser.2010.04.005.

[15] T. Tu, G.P. Rajarathnam, A.M. Vassallo, Optimization of a stand-alone photovoltaic–wind–diesel–battery system with multi-layered demand scheduling, Renew. Energy. 131 (2019) 333–347. https://doi.org/10.1016/j.renene.2018.07.029.

[16] E. Niesten, F. Alkemade, How is value created and captured in smart grids? A review of the literature and an analysis of pilot projects, Renew. Sustain. Energy Rev. 53 (2016) 629–638.

[17] T. Castillo-Calzadilla, C.M. Andonegui, M. Gomez-Goiri, A.M. Macarulla, C.E. Borges, Systematic Analysis and Design of Water Networks With Solar Photovoltaic Energy, IEEE Trans. Eng. Manag. (2019) 1–14. https://doi.org/10.1109/TEM.2019.2940340.

[18] K.R. Khalilpour, A. Vassallo, Technoeconomic parametric analysis of PV-battery systems, Renew. Energy. 97 (2016) 757–768. https://doi.org/10.1016/j.renene.2016.06.010.

[19] N. Carlisle, O. Van Geet, S. Pless, Definition of a Zero Net Energy Community, 2009.

[20] P. Augustine, The Time Is Right for Utilities to Develop Community Shared Solar Programs, Electr. J. 28 (2015) 107–108. https://doi.org/10.1016/J.TEJ.2015.11.010.

[21] H. Awad, M. Gül, Optimisation of community shared solar application in energy efficient communities, Sustain. Cities Soc. 43 (2018) 221–237. https://doi.org/10.1016/j.scs.2018.08.029.

[22] D. Feldman, A.M. Brockway, E. Ulrich, R. Margolis, Shared Solar: Current Landscape, Market Potential, and the Impact of Federal Securities Regulation, 2015. www.nrel.gov/publications. (accessed January 25, 2019).

[23] M. Shakouri, H.W. Lee, Y.-W. Kim, A probabilistic portfolio-based model for financial valuation of community solar, Appl. Energy. 191 (2017) 709–726.

[24] T. Castillo-Calzadilla, A.M. Macarulla, O. Kamara-Esteban, C.E. Borges, A case study comparison between photovoltaic and fossil generation based on direct current hybrid microgrids to power a service building, J. Clean. Prod. 244 (2020) 118870. https://doi.org/10.1016/j.jclepro.2019.118870.

[25] E. Barbour, D. Parra, Z. Awwad, M.C. González, Community energy storage: A smart choice for the smart grid?, Appl. Energy. 212 (2018) 489–497. https://doi.org/10.1016/J.APENERGY.2017.12.056.

[26] S. Freitas, C. Reinhart, M.C. Brito, Minimizing storage needs for large scale photovoltaics in the urban environment, Sol. Energy. 159 (2018) 375–389.

https://doi.org/10.1016/J.SOLENER.2017.11.011.

[27] L. He, S. Zhang, Y. Chen, L. Ren, J. Li, Techno-economic potential of a renewable energy-based microgrid system for a sustainable large-scale residential community in Beijing, China, Renew. Sustain. Energy Rev. 93 (2018) 631–641.

[28] W.L. Schram, I. Lampropoulos, W.G. van Sark, Photovoltaic systems coupled with batteries that are optimally sized for household self-consumption: Assessment of peak shaving potential, Appl. Energy. 223 (2018) 69–81.

[29] T. Khatib, A. Mohamed, K. Sopian, M. Mahmoud, A New Approach for Optimal Sizing of Standalone Photovoltaic Systems, Int. J. Photoenergy. 7 (2012). https://doi.org/10.1155/2012/391213.

[30] J. Egan, D. Finn, P.H.D. Soares, V.A.R. Baumann, R. Aghamolaei, P. Beagon, O. Neu, F. Pallonetto, J. O'Donnell, Definition of a useful minimal-set of accurately-specified input data for Building Energy Performance Simulation, Energy Build. 165 (2018). https://doi.org/10.1016/j.enbuild.2018.01.012.

[31] R. Aghamolaei, Evaluation of Supply and Demand in Building Energy Performance: Application of Retrofit Scenarios in Residential Building, Energy Eng. 116 (2019) 60–79. https://doi.org/10.1080/01998595.2019.12043339.

[32] J. Allegrini, K. Orehounig, G. Mavromatidis, F. Ruesch, V. Dorer, R. Evins, A review of modelling approaches and tools for the simulation of district-scale energy systems, Renew. Sustain. Energy Rev. 52 (2015) 1391–1404. https://doi.org/10.1016/j.rser.2015.07.123.

[33] M. Abeini Rad, Creating a Future for an Ancient Sustainable City, Yazd, (2014).

[34] SketchUp, Google SketchUp, (2018). https://www.sketchup.com/.

[35] DesignBuilder, DesignBuilder Software Ltd - Home, (2017). https://www.designbuilder.co.uk/ (accessed October 24, 2017).

[36] E. Pourazarm, A. Cooray, Estimating and forecasting residential electricity demand in Iran, Econ. Model. 35 (2013) 546–558.

[37] Statisitcal Center, Statisitcal Center of Iran, (2018). https://www.amar.org.ir/english/Statistics-by-Topic/Energy.

[38] Yazd Municipality, Master and detailed plan of Tehran, Yazd, Iran, 2009.

[39] R. Aghamolaei, Evaluation of Supply and Demand in Building Energy Performance: Application of Retrofit Scenarios in Residential Building, Energy Eng. 116 (2019) 60–79. https://doi.org/10.1080/01998595.2019.12043339.

[40] Weather, Weather Data by Location | EnergyPlus, (2017). https://energyplus.net/weather

(accessed July 3, 2017).

[41] SolarGis, Word bank Group, (2020). https://solargis.com/maps-and-gis-data/download/middle-east-and-north-africa.

[42] W. Zhou, H. Yang, Z. Fang, Battery behavior prediction and battery working states analysis of a hybrid solar?wind power generation system, Renew. Energy. 33 (2008) 1413–1423. https://doi.org/10.1016/j.renene.2007.08.004.

[43] J. Widén, E. Wäckelgård, P.D. Lund, Options for improving the load matching capability of distributed photovoltaics: Methodology and application to high-latitude data, Sol. Energy. 83 (2009) 1953–1966. https://doi.org/10.1016/j.solener.2009.07.007.

[44] B. Dunn, H. Kamath, J.-M. Tarascon, Electrical Energy Storage for the Grid: A Battery of Choices, Science (80-.). 334 (2011) 928–935. https://doi.org/10.1126/science.1212741.

[45] M.H. Shamsi, Analysis of an electric Equivalent Circuit Model of a Li-Ion battery to develop algorithms for battery states estimation, 2016.

[46] O. Tremblay, Experimental Validation of a Battery Dynamic Model for EV Applications, World Electr. Veh. J. 03 (2009).

[47] Z. Zhang, J. Wang, X. Wang, An improved charging/discharging strategy of lithium batteries considering depreciation cost in day-ahead microgrid scheduling, Energy Convers. Manag. 105 (2015) 675–684. https://doi.org/10.1016/j.enconman.2015.07.079.

[48] Y. Park, G.O. Rogers, Neighborhood planning theory, guidelines, and research: Can area, population, and boundary guide conceptual framing?, J. Plan. Lit. 30 (2015) 18–36.

[49] H. Barton, M. Grant, R. Guise, Shaping neighbourhoods : a guide for health, sustainability and vitality, Spon, 2003.

[50] S.Z. Shahraki, D. Sauri, P. Serra, S. Modugno, F. Seifolddini, A. Pourahmad, Urban sprawl pattern and land-use change detection in Yazd, Iran, Habitat Int. 35 (2011) 521–528.

[51] K. Steemers, Energy and the city: density, buildings and transport, Energy Build. 35 (2003) 3–14. https://doi.org/10.1016/S0378-7788(02)00075-0.

[52] C. Hachem, A. Athienitis, P. Fazio, Evaluation of energy supply and demand in solar neighborhood, Energy Build. 49 (2012) 335–347. https://doi.org/10.1016/j.enbuild.2012.02.021.

[53] R. Rajbongshi, D. Borgohain, S. Mahapatra, Optimization of PV-biomass-diesel and grid base hybrid energy systems for rural electrification by using HOMER, Energy. 126 (2017) 461–474. https://doi.org/10.1016/j.energy.2017.03.056.

[54] GlobalPetrolPrices, PetrolPrices, (2019).

https://www.globalpetrolprices.com/Iran/diesel_prices/.

[55] E. Román, R. Alonso, P. Ibañez, S. Elorduizapatarietxe, D. Goitia, Intelligent PV module for grid-connected PV systems, IEEE Trans. Ind. Electron. 53 (2006) 1066–1073. https://doi.org/10.1109/TIE.2006.878327.

[56] P. Lund, Large-scale urban renewable electricity schemes - Integration and interfacing aspects, in: Energy Convers. Manag., 2012: pp. 162–172. https://doi.org/10.1016/j.enconman.2012.01.037.

[57] A. Kang, K. Ivan, D. Rovas, Opportunities for Communal PVT Heating Systems with Storage, in: Eur. Conf. Comput. Constr., Crete, 2019: pp. 337–344. https://doi.org/10.35490/EC3.2019.186.

[58] K.G. Firouzjah, Assessment of small-scale solar PV systems in Iran: Regions priority, potentials and financial feasibility, Renew. Sustain. Energy Rev. 94 (2018) 267–274. https://doi.org/10.1016/j.rser.2018.06.002.

[59] BatteryUniversity, BU-1003: Electric Vehicle (EV) – Battery University, (2019). https://batteryuniversity.com/index.php/learn/article/electric_vehicle_ev (accessed June 5, 2019).

[60] R. Fu, D. Feldman, R. Margolis, M. Woodhouse, K. Ardani, U.S. solar photovoltaic system cost benchmark: Q1 2017, 2017. www.nrel.gov/publications. (accessed July 23, 2018).

Appendix A: Settlement Plan and building consumption profiles

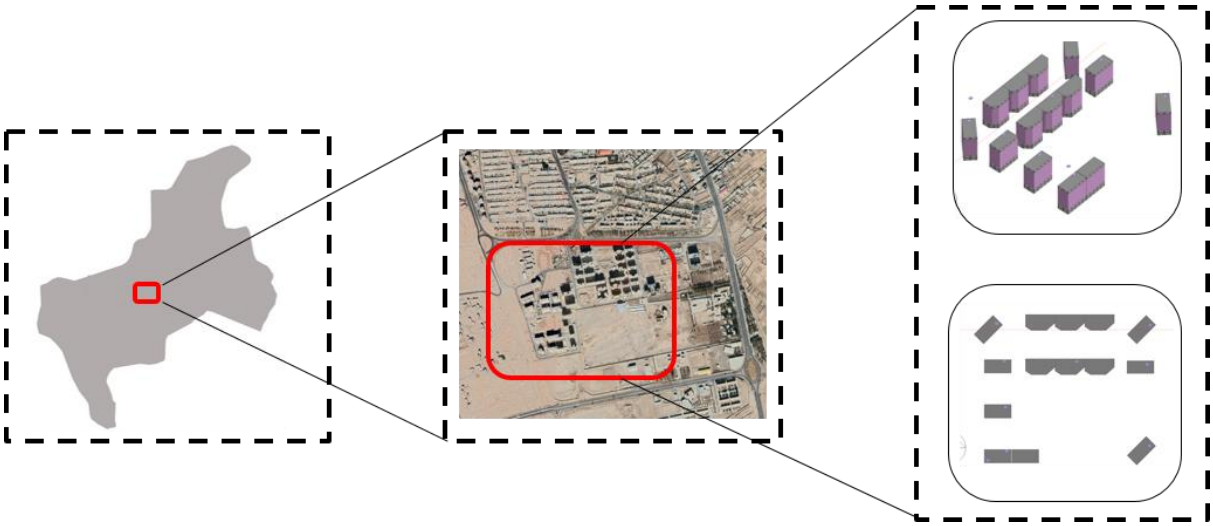

Figure 12- The location and layout of residential buildings selected as the case study of this research at the city, neighbourhood and block scales.

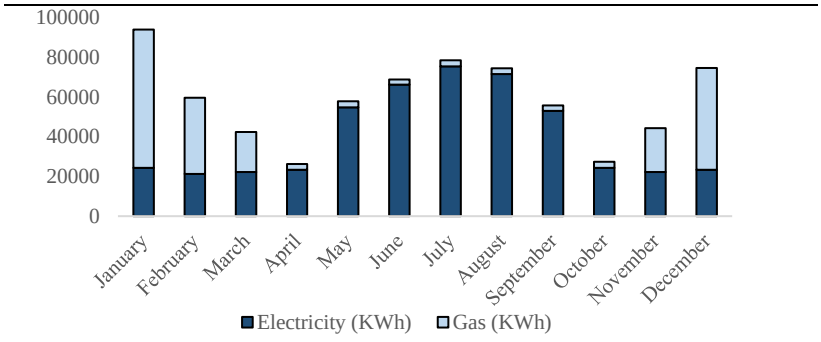

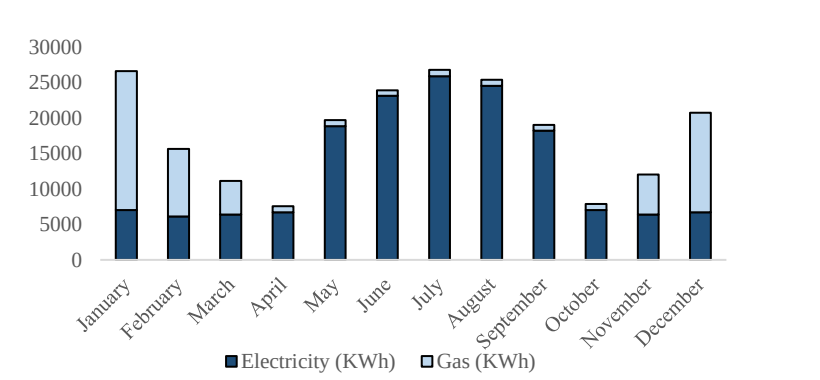

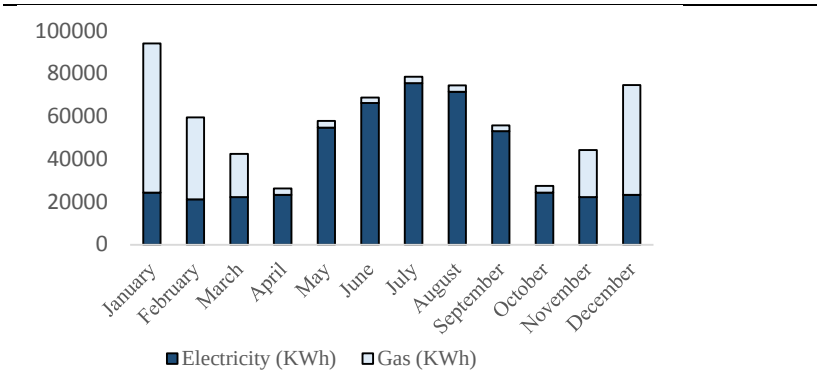

Figure 13- Monthly energy consumption profile for the apartment buildings in the residential block. The figure identifies the major end uses with heating dominating during winter and cooling dominating during summer. Lighting and DHW remain relatively constant throughout the year.

Appendix B: Modeling, configuration and sizing of the PV system

PV array: The suggested size of one PV system used in the simulation is 4 kW, which comprises 16 x 260 W panels, at 47^0C. Different sizing combinations are tested for the neighborhood. These panels are connected to produce an array with 230 V. The panel distribution on a roof depends on the size of the installed PV system and associated voltage and current requirements of the system. For instance, considering 4 kW PV system for a distributed architecture, the number of panels are decided based on the overall PV system size. A 16 kW PV system would need four PV systems of size 4 kW. Estimated capital and replacement cost of PV is 1000 USD/kW. The lifetime is assumed to be 25 years. 80% derating factor is applied to the electricity production from each PV panel [58]. The panels are modelled as fixed and tilted south at an angle equal to the latitude of the site. HOMER assumes the PV array is outfitted with a Maximum Power Point Tracker (MPPT), in which case the output of the array is effectively linear with incident solar radiation, regardless of the DC bus voltage identification of the number of panels involves the use of PV system size. For instance, PV system size (802kW; Table 2) is used to identify the number of panels required for a peak load of 253.39kW. There are different combinations possible to attain the system requirements. For instance, the 802kW (~800kW) PV system can be divided into two subsystems of 400kW each. Each 400kW subsystem can be further divided into four substations of 100kW equipped with an inverter. Hence, considering each single PV system of 4kW.

The distribution of panels for a distributed PV installation depends on the PV system size determined using the load profiles. The panels can be connected in a different arrangement to

satisfy the load requirements. Besides, the total number of panels on any roof is also limited by the available roof area. For a centralized PV installation, the panels are assumed to be centrally located in various combinations so as to satisfy the overall load requirements.

Storage: The properties of the battery remain constant throughout its lifetime and are not affected by external factors such as temperature. 100 kWh Lithium-ion batteries (rated at a nominal voltage of 600V, with a capacity of 167 Ah) storage are chosen for the analysis. In order to produce higher energy capacity, batteries are connected in series. Different combinations of these batteries are analyzed to obtain the optimum number and size. The estimated price of each battery is 20,000 USD with a replacement cost of 20,000 USD. This battery is characterized by its versatility of application and zero-maintenance design with life expectancy of 15 years [59]. Different numbers of these batteries are considered in the analysis conducted.

Converter: The converter used in the simulation is a generic system converter. The estimated capital cost of the converter is 300 USD/kW and the replacement cost is 300 USD/kW [60]. A lifetime of 20 years is assumed in which the inverter efficiency is assumed to be 95% and the converter efficiency is assumed to be 90%, for all sizes considered. The California Energy Efficiency (CEC) of the inverter is 10% at 90% load, 95% at 50% load and 95% at 100%.